

## 7. JURASSIC CALCAREOUS NANNOFOSSILS FROM PRERIFT SEDIMENTS DRILLED DURING ODP LEG 173, IBERIA ABYSSAL PLAIN, AND THEIR IMPLICATIONS FOR RIFT TECTONICS<sup>1</sup>

Andrea Concheryo<sup>2</sup> and Sherwood W. Wise Jr.<sup>3</sup>

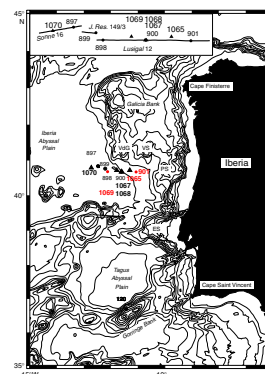
### ABSTRACT

Upper Jurassic calcareous nannofossil assemblages have been studied from strata cored over basement blocks now buried under the Iberia Abyssal Plain (Ocean Drilling Program Leg 173 Sites 1065 and 1069). The youngest Jurassic assemblages at each site are Tithonian in age, the same as those at nearby Leg 149 Site 901, an age that predates the breakup of the Iberia continental margin. The paucity of the assemblages, the prevalence of coccospheres, and the relatively high organic contents of the fine clastic sediments in which they occur are characteristic of a restricted interior basin that had little communication with the open ocean. During the major rifting episode (a Berriasian event), the Jurassic sequences were dispersed along with their underlying blocks of presumed continental crust across the ocean–continent transition of the Iberia Abyssal Plain, probably as a result of detachment faulting.

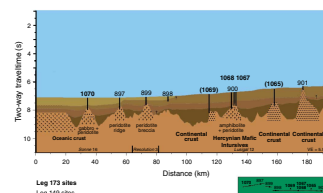
### INTRODUCTION

During Ocean Drilling Program (ODP) Leg 173, five deep sites were drilled into the Iberia Abyssal Plain (IAP) west of Portugal (Figs. F1, F2) in order to study the process of rifting and breakup of continental lithosphere on a passive, nonvolcanic margin (Whitmarsh, Beslier, Wallace,

F1. Bathymetric chart of the west Iberia margin, p. 12.



F2. Composite west to east cross section, p. 13.



<sup>1</sup>Concheryo, A., and Wise, S.W., Jr., 2001. Jurassic calcareous nannofossils from prerift sediments drilled during ODP Leg 173, Iberia Abyssal Plain, and their implications for rift tectonics. *In* Beslier, M.-O., Whitmarsh, R.B., Wallace, P.J., and Girardeau, J. (Eds.), *Proc. ODP, Sci. Results, 173, 1–24* [Online]. Available from World Wide Web: <[http://www-odp.tamu.edu/publications/173\\_SR/VOLUME/CHAPTERS/SR173\\_07.PDF](http://www-odp.tamu.edu/publications/173_SR/VOLUME/CHAPTERS/SR173_07.PDF)>. [Cited YYYY-MM-DD]

<sup>2</sup>Cat. De Paleontologia, Departamento de Ciencias Geológicas, Universidad de Buenos Aires, 1428, Buenos Aires, Argentina, South America.

<sup>3</sup>Department of Geological Sciences, 4100, Florida State University, Tallahassee FL 32306-4100, USA. [wise@gly.fsu.edu](mailto:wise@gly.fsu.edu).

Initial receipt: 19 October 1999

Acceptance: 7 December 2000

Web publication: 18 May 2001

Ms 173SR-005

et al., 1998). At two of these sites, 1065 and 1069, Jurassic sediments thought to overlie continental crust were penetrated, although neither site reached igneous or metamorphic basement. However, clastic sediments dated as Late Jurassic in age were recovered. Shipboard analysis of calcareous nannofossils suggested that these may have been deposited in a restricted interior basin that formed during an early stage of rifting (Shipboard Scientific Party, 1998c). We present here a more extended analysis of those assemblages to better document the age and environment in which they were deposited. Of interest is the spatial distribution of these Jurassic clastic sediments in relation to previously mapped Jurassic interior basins along the Iberian margin.

The assemblages encountered are similar to those described from the same area at Site 901 (de Kaenel and Bergen, 1996), where predominantly olive-black Jurassic claystones interbedded with calcareous sandstones were cored intermittently over 47.11 m with poor recovery (13%). The clastic lithologies strongly suggest that the site is underlain by continental crust. The most abundant nannofossil assemblages were found in a few thin streaks of nannofossil ooze within the claystones (E. de Kaenel, pers. comm., 1997). These were dated as late Tithonian in age by de Kaenel and Bergen (1996), who found *Rotelapillus laffitei* and *Crucellipsis cuvillieri* in the uppermost sample along with *Stephanolithion bigotii*. *R. laffitei* had not been found previously to co-occur with *S. bigotii*, although Wind (1978, fig. 1) suggested that it might. Wind (1978, p. 764) also noted discrepancies among various authors in the placement of the first occurrence of *C. cuvillieri* (above and below the Tithonian/Berriasian boundary), which he attributes to different concepts of the morphological variation within the species.

Bralower et al. (1989) placed the extinction of *S. bigotii* close to the Kimmeridgian/Tithonian boundary, prior to the appearance of *Conusphaera mexicana mexicana*. Wind (1978, fig. 3), however, had recorded their overlap in one Tithonian sample from Deep Sea Drilling Project (DSDP) Hole 391C; thus, the presence of *S. bigotii* in some abundance along with *C. mexicana* throughout the section at Site 901 is noteworthy. De Kaenel and Bergen (1996) considered reworking an unlikely explanation for the presence there of *S. bigotii* and suggested that its extinction was possibly ecologically controlled. Specifically, they noted that it overlapped the range of *Stephanolithion atmetros* in northwest Europe (Bown et al., 1988) and that both taxa were present in Hole 901A. *Stephanolithion*, they reasoned, could range higher in Boreal outcrop sections as well as at Site 901, which showed some other Boreal influences despite a marked Tethyan assemblage composition in many respects (such as the presence of *Conusphaera*).

More recently, Bown and Cooper (1998, p. 52) reported the last occurrence (LO) of *S. bigotii* near the lower/middle Tithonian boundary (polarity Chron CM20r) in DSDP Site 534 (Blake-Bahama Basin), well above its occurrence in the classical Kimmeridgian sequences of England. Confirmation of the range of *S. bigotii* in the study area, therefore, is pertinent to understanding the relationships discussed above.

Another problematic taxon noted by de Kaenel and Bergen (1996) within their Tithonian section was *Lotharingius sigillatus*. Although this taxon was also thought to have an Oxfordian extinction (Bown et al., 1988; Bown and Cooper, 1998), de Kaenel and Bergen (1996, p.29) surmised that it may well be in situ in their Cores 149-901A-5R to 7R.

Beyond the IAP, a detailed study of Jurassic calcareous nannofossils in outcrops of onshore Portugal has been conducted by J. Bergen (unpubl. data). None of his sections, however, extends above the lower-

most Kimmeridgian as Jurassic calcareous nannofossils are absent in Portugal above that level.

## **METHODS**

Unless otherwise noted, the abundances of calcareous nannofossils were tabulated from standard smear slides made from raw sediment. These were examined under a Zeiss Axioskop at 1000× magnification. Seven levels of abundance were recorded according to the following scheme:

- P = present (1 specimen per 201–500 fields of view).
- R = rare, (1 specimen per 51–200 fields of view).
- F = few, (1 specimen per 11–50 fields of view).
- C = common, (1 specimen per 2–10 fields of view).
- A = abundant, (1–10 specimens per field of view).

The same definitions were used to estimate total abundance of each sample except that “VR” (very rare) was used in place of “P”, and “B” was used to indicate a barren sample.

Estimates of preservation are based on the scheme of Roth and Thierstein (1972), as follows:

- P = poor, severe dissolution, fragmentation, and/or overgrowth have occurred; most primary features have been destroyed and many specimens cannot be identified at the specific level.
- M = moderate, dissolution and/or overgrowth are evident; a significant proportion (up to 25%) of the specimens cannot be identified to species level with absolute certainty.
- G = good, little dissolution and/or overgrowth is seen; diagnostic characteristics are preserved and all specimens can be identified.
- E = excellent, no dissolution and/or overgrowth is observed; all specimens can be identified.

Taxa considered in this report are listed in the “[Taxonomic Appendix](#),” p. 11, where they are arranged alphabetically by generic epithets. Bibliographic references for these species are given in Perch-Nielsen (1985), de Kaenel and Bergen (1996), and Bown (1998).

## **SITE SUMMARIES AND BIOSTRATIGRAPHY**

### **Site 1065**

Hole 1065A was drilled in 5412 m of water with the intention of reaching a tilted fault block to determine whether the block consisted of continental crust or not. An ancillary objective was to date any pre-rift or synrift sediment overlying basement.

More than 322 m of Jurassic clays, claystones, and dolomitic claystones was cored, although basement was not reached. The sequence was subdivided into two subunits. Dark greenish gray to medium dark gray soft clay dominates lithologic Subunit VA (308.8 to 501.5 meters below seafloor [mbsf]), whereas Subunit VB (501.5–631.4 mbsf) consists of claystone, some of which is dolomitic. Turbidites, some consisting of

sandstones and conglomerates, are minor constituents. These lithologies represent primarily offshore, sub-wave base suspension deposits (Shipboard Scientific Party, 1998a).

Core recovery was poor (<5%) in this portion of the hole, and no nannofossil ooze was encountered. Assemblages, therefore, were highly diluted by the clastic sediments. The presence of much fine silt made it difficult to concentrate the nannofossils by gravitational settling techniques.

The stratigraphic distribution of nannofossils in Cores 173-1065A-8R to 35R is given in Table T1; the fossils are illustrated by light micrographs in Plates P1, P2, and P3. Their overall abundance ranges from few to very rare and their preservation from poor to good, with the best preservation in Cores 1065A-8R to 20R. No overgrowths were noted; only dissolution affected the preservation of the specimens.

*S. bigotii* is present down to Core 173-1065A-20R, and *Conusphaera mexicana minor* along with small specimens of *C. mexicana mexicana* (4–5 µm) were traced down to Core 173-1065A-13R. Among the other taxa present are *Zeugrhabdotus erectus*, *Zeugrhabdotus embergeri*, *Miravetesina favula*, *Diazomatolithus lehmanii*, and *Diazomatolithus galicianus*. The latter was described as new from Hole 901A by de Kaenel and Bergen (1996), but it has not been recorded outside of this region. The only taxa noted as common in Table T1 belong to the Watznaueriaceae. These include members of the *Ellipsagelosphaera/Watznaueria* plexus, in which the *Watznaueria* are dominant. Cores 173-1065A-21R to 31R are barren of nannofossils.

There are rare to very rare occurrences of nannofossils from Section 173-1065A-32R-CC to the bottom of the hole consisting only of dissolution-resistant members of the Watznaueriaceae in which *Watznaueria* remains dominant. Unlike the well-preserved members of this plexus noted higher in the hole, however, these specimens exhibit mostly broken or fragmented shields.

Cores 173-1065A-8R to 20R are clearly no younger than Tithonian in age, based on the presence of *S. bigotii* and *Discorhabdus patulus* in the absence of lower Berriasian index taxa such as *Nannococcus steinmannii*, *Retacapsa angustiforata*, and *Assipetra infracretacea* (see Bergen, 1994). An age no older than Tithonian for the upper portion of the section is indicated by the presence of *C. mexicana mexicana* and *C. mexicana minor* in Cores 173-1065A-10R to 13R (Bown and Cooper, 1998: fig. 4.2). *C. mexicana minor* is confined to the lower Tithonian in the distribution charts of Bralower et al. (1989) but ranges into the upper Tithonian in that of de Kaenel and Bergen (1996) (Table T2) for Hole 901A. The presence of conusphaerids of only five µm or less in length would suggest that top of the Jurassic section in Hole 1065A (Cores 173-1065A-10 to 13) belongs to the lower to mid-Tithonian (see "Discussion," p. 5).

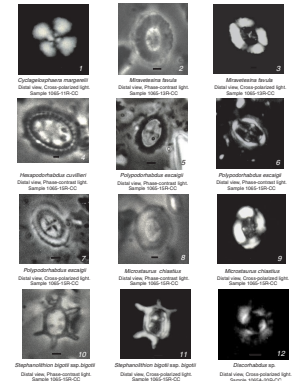
Below the barren interval from Cores 173-1065A-21R to 31R, watznauerids continue to dominate the ellipsagelospherids, which could indicate a Tithonian age (J. Bergen, pers. comm, 1997). The paucity of nannoliths in this interval, however, makes any such determination highly speculative.

**Site 1069**

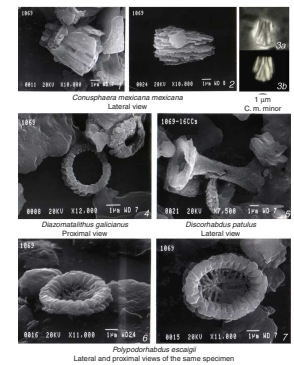
Hole 1069A was drilled in 5075 m of water within the ocean-continent transition (OCT) to determine the nature of a relatively flat-topped, north-south basement ridge buried under postrift sediments (Figs. F1, F2). Jurassic clastic sediments were encountered at 867.83

**T1.** Stratigraphic distribution of calcareous nannofossils, Hole 1065A, p. 17.

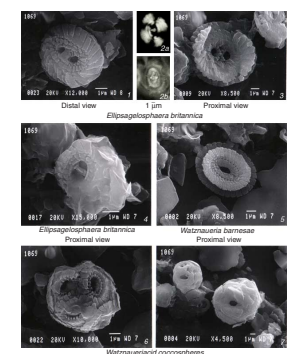
**P1.** Light micrographs of calcareous nannofossils, Hole 1065A, p. 20.



**P2.** Scanning electron micrographs showing conusphaerids' inner cores, p. 21.



**P3.** Scanning electron micrographs of nannofossils showing a range of preservations, p. 22.



**T2.** Stratigraphic distribution of calcareous nannofossils, Hole 1069A, p. 18.

mbsf where a 10-cm-thick medium dark clay (lithologic Subunit VA) was recovered at the base of Core 173-1069A-16R (Fig. F3). Beneath that level core recovery was poor (<3%), with only a series of limestone and low-grade metamorphic cobbles retrieved without any fine-grained matrix (Subunit VB, >85.65 m thick). Nonetheless, these rocks indicated that the basement at this locality was most certainly continental (Shipboard Scientific Party, 1998b).

Although the cores from Subunit VB were barren of nannofossils, the dark clay in Subunit VA did contain a thin (2 cm thick) light gray nannofossil ooze, the only such concentration of Jurassic coccoliths recovered on this cruise. These provided the opportunity to obtain scanning electron microscope (SEM) images of the assemblage (Pls. P2, P3) along with light micrographs (Pls. P4, P5).

The thin streak of nannofossil ooze was recorded in Sample 173-1069A-16R-3, 129 cm. It contains an assemblage generally similar to that in Cores 8R to 20R at Site 1065 except that more delicate, less dissolution-resistant forms such as *Stradnerlithus sexiramatus* are present and *C. mexicana mexicana* is much larger in size (Table T2). In the SEM, some specimens exhibit some dissolution, whereas others show minor overgrowth by secondary calcite. *S. bigotiis* also present along with *D. galicianus*, *C. cuvillieri*, *Hexapodorhabdus cuvillieri*, *Paleopontosphaera erismata*, *D. patulus* (= *Podorhabdus grassei* of authors), and *Tubirhabdus patulus*. Complete coccospheres belonging to various taxa are common (Pl. P2, figs. 6, 7).

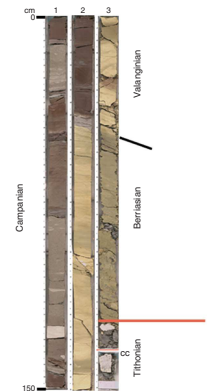
Of these forms, *H. cuvillieri*, *S. bigotii*, *D. patulus*, and *T. patulus* indicate an age no younger than Tithonian, whereas the presence of *C. mexicana mexicana* requires an age assignment no older than Tithonian. As discussed for Site 1065 above, the range charts of most authors indicate an early Tithonian age for this assemblage; however, all of these taxa range into the upper Tithonian at Site 901 as delimited by de Kaenel and Bergen (1996, table 2; fig. 2). The presence of *C. cuvillieri* and *Umbria granulosa* ssp. *minor* indicates a placement very close to the top of the Tithonian according to the biostratigraphic summary tables of Bralower et al. (1989, fig. 14) and Bown and Cooper (1998, fig. 4.2). As noted previously, there are varying taxonomic concepts in the literature for *C. cuvillieri*, and there does not yet seem to be a consensus as to the correlation of its first occurrence with respect to the Jurassic/Cretaceous boundary.

A single specimen of *Diadorhombus rectus*, whose first occurrence (FO) is considered to be in the Berriasian (Lower Cretaceous) (e.g., see Bralower et al, 1989, fig. 14), was noted by one of us but not photographed. We consider this to be a downhole contaminant. Because the Tithonian ooze lamina is very thin (2 mm) and only lies a few centimeters below the subjacent upper Berriasian chalk (Fig. F3), downhole contamination is possible.

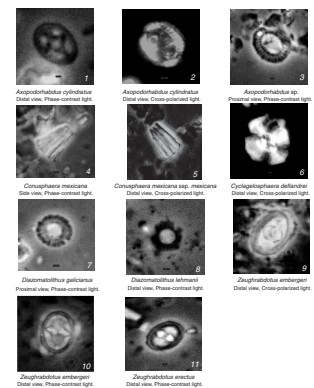
## DISCUSSION

The overlap in the ranges of *S. bigotii* and the two subspecies of *C. mexicana* is clearly demonstrated in our two drill sites in the IAP, thereby confirming the co-occurrence of these taxa as suggested by Wind (1978) for the western Atlantic and in the Iberian region by de Kaenel and Bergen (1996) (see also Bown and Cooper, 1998, fig. 4.2). Such an overlap reliably indicates the presence of Tithonian-age sediments in our study area. Nonetheless, Bown and Cooper (1998, p. 47)

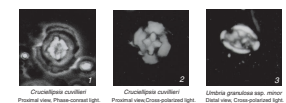
F3. Tithonian dark gray clastic clay in Core 173-1069A-16R, p. 14.



P4. Light micrographs of calcareous nannofossils, p. 23.



P5. Light micrographs of *C. cuvillieri* and *U. granulosa* ssp. *minor*, p. 24.



note that "*S. bigotii bigotii* appears to have a diachronous LO," and one must be wary of the fact that the Galicia interior basin was actively subsiding at this time as a result of minor rifting or stretching of the lithosphere, thus the possibility of reworking of nannofossils from older strata was a distinct possibility. The fact that the central structure of this taxon, however, is rather delicate, that the specimens are well preserved (some with exceptionally long central spines), and that they are relatively uncommon to begin with in most Upper Jurassic sequences leads us to consider reworking in this instance unlikely (as did de Kaenel and Bergen, 1996).

*C. mexicana minor* in the presence of very small (4 to 5  $\mu\text{m}$ ) *C. mexicana mexicana* in Cores 173-1065A-10R to 13R suggests that the interval is early to mid Tithonian in age. Bralower et al. (1989) found that a number of Jurassic evolutionary lineages begin with very small forms (to which they give the subspecies designation of *minor*) that eventually develop to a larger size. They further suggest that this size progression may have biostratigraphic utility. Given the uniformly small size of the Hole 1065A conusphaerid assemblage, an assignment to the lower to mid Tithonian seems appropriate (see, however, further discussion of this assemblage in relation to its restricted environment below). This section, therefore, is older than that sampled at Site 1069, where full-length ( $\sim 8 \mu\text{m}$ ) specimens of *C. mexicana mexicana* are present.

Some of the specimens of *C. mexicana* in Hole 1065A, however, exhibit a peculiar diverging, if not crossing, pattern reminiscent of the Cretaceous *C. rothii* (e.g., Pl. P2, Fig. 3). The Hole 1065A specimens, however, are considerably smaller than typical *C. rothii*, measuring only 4 to 5  $\mu\text{m}$  or less as mentioned above. Thus, these are not assigned to that species here. Whether the *C. rothii* diagonal cross-hatched pattern actually originated in the Tithonian is an interesting question for further research.

As noted previously, the predominantly fine-grained Jurassic clastic sediments at Site 1065 were deposited below wave base. Basin restriction at that site is indicated by the paucity of calcareous nannofossils, the general lack of bioturbation, and relatively high organic contents (up to 0.9%) (Shipboard Scientific Party, 1998b: table 7). Thin streaks of nannofossil ooze only a millimeter or two thick at Sites 901 and 1069 are the only indications of brief communications of this basin with the open ocean. These thin laminae of nannofossil ooze, which indicate enhanced nannoplankton productivity in the surface waters, were preserved because of the general absence of bioturbation at the sediment/water interface. They therefore indicate intervals when well-oxygenated surface waters existed above dysaerobic bottom waters.

One other characteristic of dysaerobic or anoxic bottom-water conditions is the presence of common nannofossil coccospheres, such as those illustrated in Plate P3, Figures 6 and 7. An occurrence analogous to this has been described by Gallois and Medd (1979: pl. 1, fig. d), who noted high abundances of *Ellipsogellosphaera* coccospheres in thin chalk laminations (bands) of the Kimmeridgian Clay "black shales" of England.

The restricted nature of the basin in our study area raises the question as to whether the small size of the Hole 1065A conusphaerids discussed above might actually be due to environmental factors rather than to evolutionary development. Erba et al. (1995) described dwarf nannofossil assemblages from Campanian lagoonal deposits of Wodejebato Guyot in the central Pacific Ocean (ODP Sites 873, 874, and 877), which they attributed to restricted environmental conditions. They pre-

sented biometric measurements for seven members of their assemblages, noting that the average sizes were about half that of normal oceanic assemblages of the same age at nearby Site 869. Among the Upper Cretaceous taxa they measured is *Watznauria barnesae*, a long-ranging form that also occurs in our Jurassic assemblages. We therefore made similar biometric measurements of that taxon in our Site 1065A material (Sample 173-1065A-11-CC) and compared our results with those of Erba et al. (1995: table 8) in our Table T3. We find that our Hole 1065A *W. barnesae* specimens match in size those of Erba et al.'s (1995) normal oceanic assemblage specimens, rather than those of their dwarf (lagoonal) floras, which suggests that our small Jurassic conusphaerids are indeed the products of early evolutionary development rather than environmental restriction.

Although we interpret the age of the nannofossil assemblages discussed here as Tithonian, as noted previously those in the thin lamina sampled at Site 1069 do contain a single specimen of an Early Cretaceous form, *Diadorhombus rectus*, which we consider to be a downhole contaminant. If this specimen is in place, however, then basin restriction in this area would have clearly continued into the earliest Cretaceous, which it may have done anyway. Lower to middle Berriasian sediments have not been identified at any site in the study region; thus, this part of the record is missing, probably as a result of erosion associated with tectonic activity. Major rifting that ventilated the basin was underway at least by the late Berriasian, as recorded by the slumped chalk unit immediately above the Tithonian at Site 1069 (Fig. F3) (see Whitmarsh, Beslier, Wallace, et al., 1998; Wise et al., 1999; Wilson et al., in press).

Although drilling was terminated before the basement was reached, 323 m of Upper Jurassic sediments was penetrated at Site 1065, indicating that the basin was undergoing significant subsidence. This, plus the other features discussed above, would fit the model of an interior basin formed during an early phase of rifting, as has been postulated for the Galicia Basin (Fig. F4) (see discussion by Pinheiro et al., 1996, and Shipboard Scientific Party, 1998a, p.8). Although Pinheiro et al. (1996: fig. 5) illustrated the Jurassic clastic sediments of Leg 149 Site 901 as an offshoot of that basin, it is difficult to envision this basin extending as far west as Leg 173 Sites 1065 and 1069.

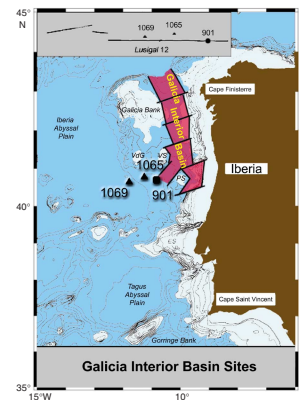
ODP Leg 173 was designed to test a variety of models that had been proposed since Leg 149 for lithospheric rifting and the formation of the OCT on the west Iberia margin. Of those discussed by the Shipboard Scientific Party (1998a, pp. 15–19), we believe that the simplest model to explain the dispersal of Jurassic sediments from a restricted interior basin originally aligned with or lying within the Galicia interior basin is the model of detachment faulting proposed by Krawczyk et al. (1996). Although a simplified model, we find it readily adaptable to explain the dispersion of remnants of our postulated Jurassic interior basin from east to west over the OCT (Fig. F5). A more sophisticated detachment-fault model for the IAP has recently been proposed by Manatschal and Frotzheim (1999).

## CONCLUSIONS

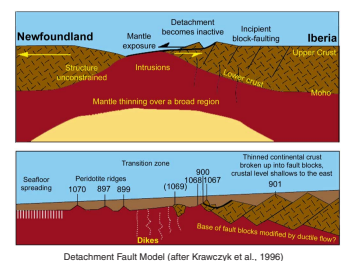
Upper Jurassic calcareous nannofossils are present at ODP Leg 173 Sites 1065 and 1069, where they overlie presumed continental basement blocks now buried under the IAP. The youngest Jurassic assem-

T3. Size variations of *Watznauria barnesae*, p. 19.

F4. Locations of sites with Jurassic clastic sediments, p. 15.



F5. Simplified model to account for the dispersion of sites with Jurassic clastic sediments, p. 16.



Detachment Fault Model (after Krawczyk et al., 1996)

blages at each site are Tithonian in age, the same as those at nearby Leg 149 Site 901. Those at Site 1065 are the oldest (early to mid-Tithonian in age), whereas those at Sites 901 and 1069 are latest Tithonian in age, having been deposited close to the Jurassic/Cretaceous boundary.

The paucity of the assemblages, the prevalence of coccospheres, and the relatively high organic contents of the fine-clastic sediments in which they occur are characteristic of a restricted interior basin, which in this case had little communication with the open ocean until the latest Tithonian, when the first nannofossil oozes appear as thin laminae (less than ~2 mm thick) at Sites 901 and 1165. These provide the first hints of better communication with the open sea; the bottom sediments, however, remained dysaerobic.

The restricted interior basin was shattered during the major rifting episode (a Berriasian event), during which sustained open marine conditions were established, resulting in the deposition of nannofossil chalks. As a consequence of this rifting, the Jurassic sequences were dispersed along with their underlying basement blocks of presumed continental crust across the ocean-continent transition of the IAP, probably as a result of detachment faulting.

## **ACKNOWLEDGMENTS**

We thank Drs. Elisabetta Erba, Paul R. Bown, and Robert Whitmarsh for their thoughtful and careful critical reviews of this paper and acknowledge with pleasure our ODP Leg 173 colleagues and co-chief scientists for many helpful discussions. Dr. Paul Wallace and the ODP staff most expeditiously provided many items necessary for the study. Discussions with Drs. Gianreto Manatschal and Nikolaus Froitzheim aboard ship and on a field trip they led to view detachment faults in the Swiss Alps following the Leg 173 postcruise meeting were especially instructive and insightful. This study was supported by USSAC funds. The first author thanks the Consejo Nacional de Investigaciones Cientificas y Técnicas-CONICET (Argentina) for facilitating her study-in-residence in Tallahassee. We thank David Davenport for his skillful execution of the figures and Kristeen Roessig and Bryan Ladner for helpful assistance in manuscript preparation. Laboratory facilities were supported by NSF grant OPP-9422893.

## REFERENCES

- Bergen, J.A., 1994. Berriasian to early Aptian calcareous nannofossils from the Vocontian Trough (SE France) and Deep Sea Drilling Site 534: new nannofossil taxa and a summary of low-latitude biostratigraphic events. *J. Nannoplankton Res.*, 16:59–69.
- Bown, P.R. (Ed.), 1998. *Calcareous Nannofossil Biostratigraphy*: London (Kluwer Academic).
- Bown, P.R., and Cooper, M.K.E., 1998. Jurassic. In Bown, P.R. (Ed.), *Calcareous Nannofossil Biostratigraphy*: London (Kluwer Academic), 34–85.
- Bown, P.R., Cooper, M.K.E., and Lord, A.R., 1988. A calcareous nannofossil biozonation scheme for the early to mid Mesozoic. *Newsl. Stratigr.*, 20:91–114.
- Bralower, T.J., Monechi, S., and Thierstein, H.R., 1989. Calcareous nannofossil zonation of the Jurassic-Cretaceous boundary interval and correlation with the geomagnetic polarity timescale. *Mar. Micropaleontol.*, 14:153–235.
- de Kaenel, E., and Bergen, J.A., 1996. Mesozoic calcareous nannofossil biostratigraphy from Sites 897, 899, and 901, Iberia Abyssal Plain: new biostratigraphic evidence. In Whitmarsh, R.B., Sawyer, D.S., Klaus, A., and Masson, D.G. (Eds.), *Proc. ODP, Sci. Results*, 149: College Station, TX (Ocean Drilling Program), 27–59.
- Erba, E., Watkins, D., and Mutterlose, J., 1995. Campanian dwarf calcareous nannofossils from Wodejebato Guyot. In Haggerty, J.A., Premoli Silva, I., Rack, F., and McNutt, M.K. (Eds.), *Proc. ODP, Sci. Results*, 144: College Station, TX (Ocean Drilling Program), 141–156.
- Gallois, R.W., and Medd, A.W., 1979. Coccolith-rich marker bands in the English Kimmeridge Clay. *Geol. Mag.*, 116:247–334.
- Krawczyk, C.M., Reston, T.J., Beslier, M.-O., and Boillot, G., 1996. Evidence for detachment tectonics on the Iberia Abyssal Plain rifted margin. In Whitmarsh, R.B., Sawyer, D.S., Klaus, A., and Masson, D.G. (Eds.), *Proc. ODP, Sci. Results*, 149: College Station, TX (Ocean Drilling Program), 603–615.
- Manatschal, G., and Froitzheim, N., 1999. Detachment faulting along non-volcanic margins: insights from the Iberia Abyssal Plain. In *Non-volcanic Rifting of Continental Margins: a Comparison of Evidence from Land and Sea: Abstracts of Talks and Posters*. Marine Studies Group/Tectonic Studies Group Discussion Meeting, 31.
- Perch-Nielsen, K., 1985. Mesozoic calcareous nannofossils. In Bolli, H.M., Saunders, J.B., and Perch-Nielsen, K. (Eds.), *Plankton Stratigraphy*: Cambridge (Cambridge Univ. Press), 329–426.
- Pinheiro, L.M., Wilson, R.C.L., Pena dos Reis, R., Whitmarsh, R.B., and Ribeiro, A., 1996. The western Iberia Margin: a geophysical and geological overview. In Whitmarsh, R.B., Sawyer, D.S., Klaus, A., and Masson, D.G. (Eds.), *Proc. ODP, Sci. Results*, 149: College Station, TX (Ocean Drilling Program), 3–23.
- Roth, P.H., and Thierstein, H., 1972. Calcareous nannoplankton: Leg 14 of the Deep Sea Drilling Project. In Hayes, D.E., Pimm, A.C., et al., *Init. Repts. DSDP*, 14: Washington (U.S. Govt. Printing Office), 421–485.
- Shipboard Scientific Party, 1998a. Leg 173 introduction. In Whitmarsh, R.B., Beslier, M. O., Wallace, P.J., et al., *Proc. ODP, Init. Repts.*, 173: College Station, TX (Ocean Drilling Program), 7–23.
- , 1998b. Site 1065. In Whitmarsh, R.B., Beslier, M.-O., Wallace, P.J., et al., *Proc. ODP, Init. Repts.*, 173: College Station, TX (Ocean Drilling Program), 65–104.
- , 1998c. Site 1069. In Whitmarsh, R.B., Beslier, M.-O., Wallace, P.J., et al., *Proc. ODP, Init. Repts.*, 173: College Station, TX (Ocean Drilling Program), 219–263.
- Whitmarsh, R.B., Beslier, M.-O., Wallace, P.J., et al., 1998. *Proc. ODP, Init. Repts.*, 173: College Station, TX (Ocean Drilling Program).
- Wilson, R.C.L., Monatschal, G., Wise, S.W., and Urquarht, E., in press. The timing, duration and location of rifting along cold passive margins: evidence from the Mesozoic of the eastern Atlantic and the Alps. *Geol. Soc. London Spec. Pap.*

- Wind, F.H., 1978. Western North Atlantic Upper Jurassic calcareous nannofossil biostratigraphy. In Benson, W.E., Sheridan, R.E., et al., *Init. Repts. DSDP*, 44: Washington (U.S. Govt. Printing Office), 761–773.
- Wise, S.W., Bernoulli, D., Manatschal, G., Rubenach, M.J., Urquhart, E., and Wilson, R.C., 1999. Chronology of rifting, Western Iberian Margin: constraints from paleontology and sedimentology, ODP Leg 173. In *Non-volcanic Rifting of Continental Margins: a Comparison of Evidence from Land and Sea: Abstracts of Talks and Posters*. Marine Studies Group/Tectonic Studies Group Discussion Meeting, 5.

## TAXONOMIC APPENDIX

### Species List by Generic Epithet

- Axopodorhabdus cylindratus* (Noël, 1965) Wind and Wise in Wise and Wind, 1977  
*Axopodorhabdus* sp.  
*Conusphaera mexicana* Trejo, 1969 ssp. *mexicana* Bralower 1989  
*Conusphaera mexicana* Trejo, 1969 ssp. *minor* Bralower ex Bown and Cooper, 1989a  
*Corollithion* sp.  
*Crepidolithus crassus* (Deflandre in Deflandre and Fert, 1954) Noël, 1965  
*Crepidolithus* sp.  
*Cruciellipsis cuvillieri* Manivit, 1966  
*Cyclagelosphaera deflandrei* Manivit, 1966  
*Cyclagelosphaera margerelii* Noël, 1965  
*Cyclagelosphaera tubulata* (Grün and Zweili, 1980) Cooper, 1987  
*Diadorhombus rectus* Worsley, 1971  
*Diazomatholithus galicianus* de Kaenel and Bergen, 1996  
*Diazomatholithus lehmanii* Noël, 1965  
*Discorhabdus corollatus* Noël, 1965  
*Discorhabdus ignotus* (Górka, 1957) Perch-Nielsen, 1968  
*Discorhabdus patulus* (Deflandre in Deflandre and Fert, 1954) Noël, 1965  
*Discorhabdus* sp.  
*Ellipsagelosphaera britannica* (Stradner, 1963) Perch-Nielsen, 1968  
*Ellipsagelosphaera reinhardtii* (Rood, Hay and Barnard, 1971) Noël, 1973  
*Ethmorhabdus gallicus* Noël, 1965  
*Hexapodorhabdus cuvillieri* Noël, 1965  
*Lotharingius sigillatus* (Stradner, 1961) Prins in Grün, Prins, and Zweili, 1974  
*Microstaurus chiasmus* (Worsley, 1971) Grün in Grün and Allemann, 1975  
*Microstaurus quadratus* Black, 1971  
*Microstaurus* sp.  
*Miravetesina favula* Grün in Grün and Allemann, 1975  
*Paleopontosphaera dubia* Noël, 1965  
*Paleopontosphaera erismata* Wind and Wise in Wise and Wind, 1977  
*Polypodorhabdus* sp.  
*Polypododrhabdus escaigii* Noël, 1965  
*Stephanolithion bigotii* Deflandre, 1939  
*Stradnerlithus sexiramatus* (Pienaar, 1969) Perch-Nielsen, 1984  
*Thoracosphaera* sp. de Kaenel and Bergen, 1996  
*Tranolithus incus* de Kaenel and Bergen, 1996  
*Tubirhabdus patulus* Prins, 1969 ex Rood, Hay and Barnard, 1973  
*Umbria granulosa* spp. *minor* Bralower and Theirstein in Bralower, Monechi, and block Thierstein, 1989  
*Watznaueria barnesae* (Black in Black and Barnes, 1959) Perch-Nielsen, 1968  
*Watznaueria barnesae* (coccosphere)  
*Watznaueria biporta* Bukry, 1969  
*Watznaueria fossacincta* (Black, 1971) Bown in Bown and Cooper, 1989b  
*Watznaueria manivita* Bukry, 1973  
*Watznaueria ovata* Bukry, 1969  
*Zeugrhabdotus embergeri* (Noel, 1959) Perch-Nielson, 1984  
*Zeugrhabdotus erectus* (Deflandre in Deflandre and Fert, 1954) Gartner, 1968  
*Zeugrhabdotus* sp.

Figure F1. Bathymetric chart of the west Iberia margin (contours at 200, 500, 1000, 1500 through 5500 m). Leg 149 sites are shown by solid circles. Sites drilled during Leg 173 are shown by solid triangles. Sites with Jurassic clastic sediments are in red. VdG = Vasco da Gama Seamount, VS = Vigo Seamount, PS = Porto Seamount, ES = Estremadura Spur. Inset shows locations of drill sites relative to three seismic reflection profiles used to create the composite section in Figure F2, p. 13 (after Shipboard Scientific Party, 1998a, fig. 1).

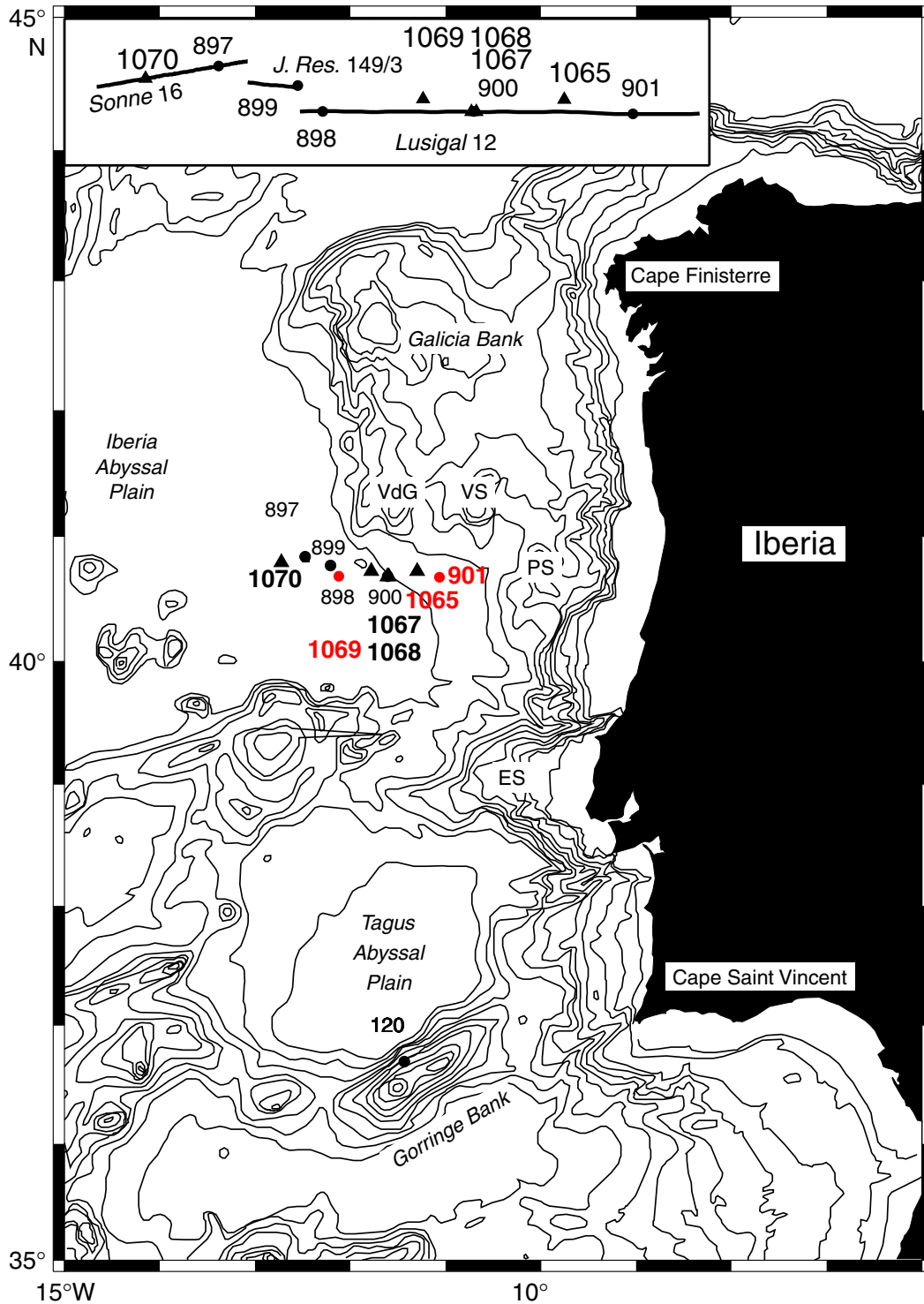


**Figure F2.** Composite west to east (left to right) cross section through the Leg 149 and Leg 173 drill sites along the tracks shown in inset from Figure F1, p. 12 (lower right). Leg 173 sites are in bold. Sites in parentheses are offset a short distance from the profile. Depth and extent of patterns are diagrammatic. Solid triangles = gabbro and amphibolite + = peridotite (after Shipboard Scientific Party, 1998a, fig. 3).

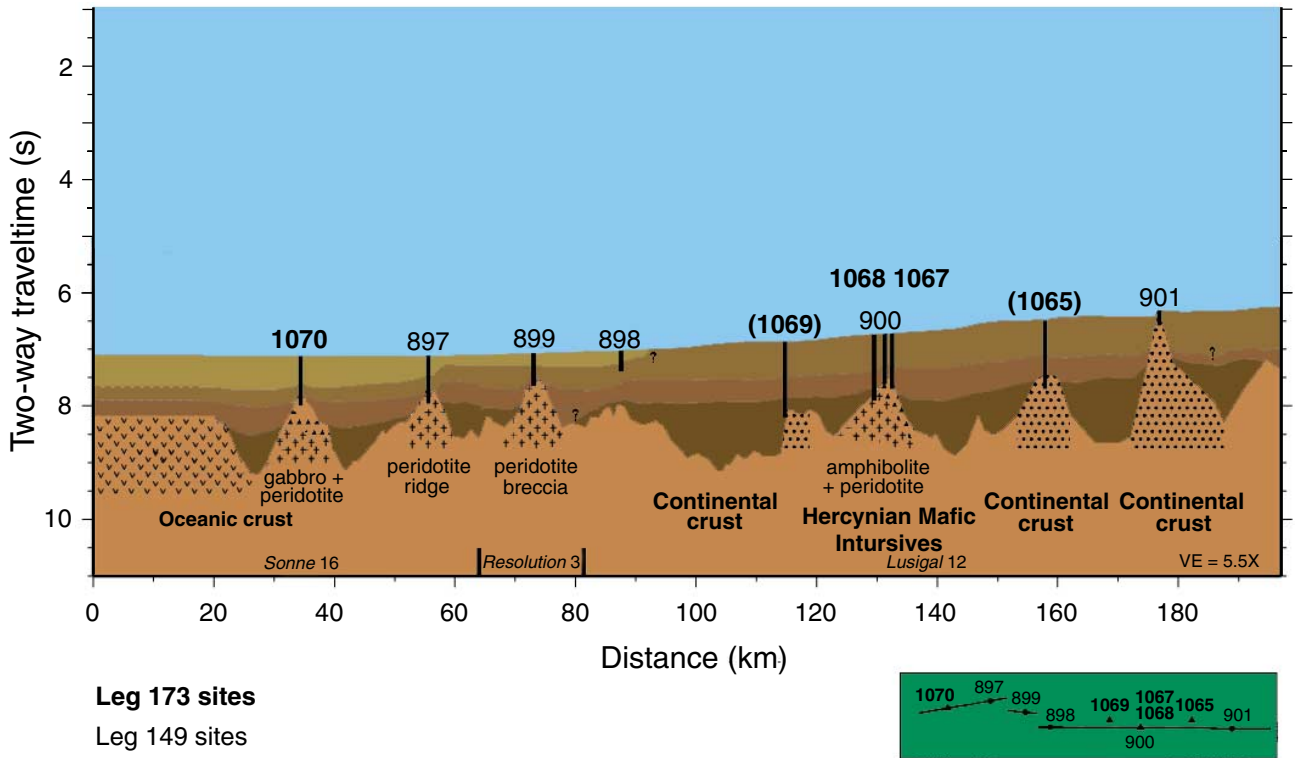


Figure F3. Core 173-1069A-16R showing Tithonian dark gray clastic clay at the bottom of Section 3 and in the core catcher (CC) overlain unconformably by slumped Berriasian chalk, then by normally bedded yellow Valanginian chalk, and reddish Campanian turbidites.

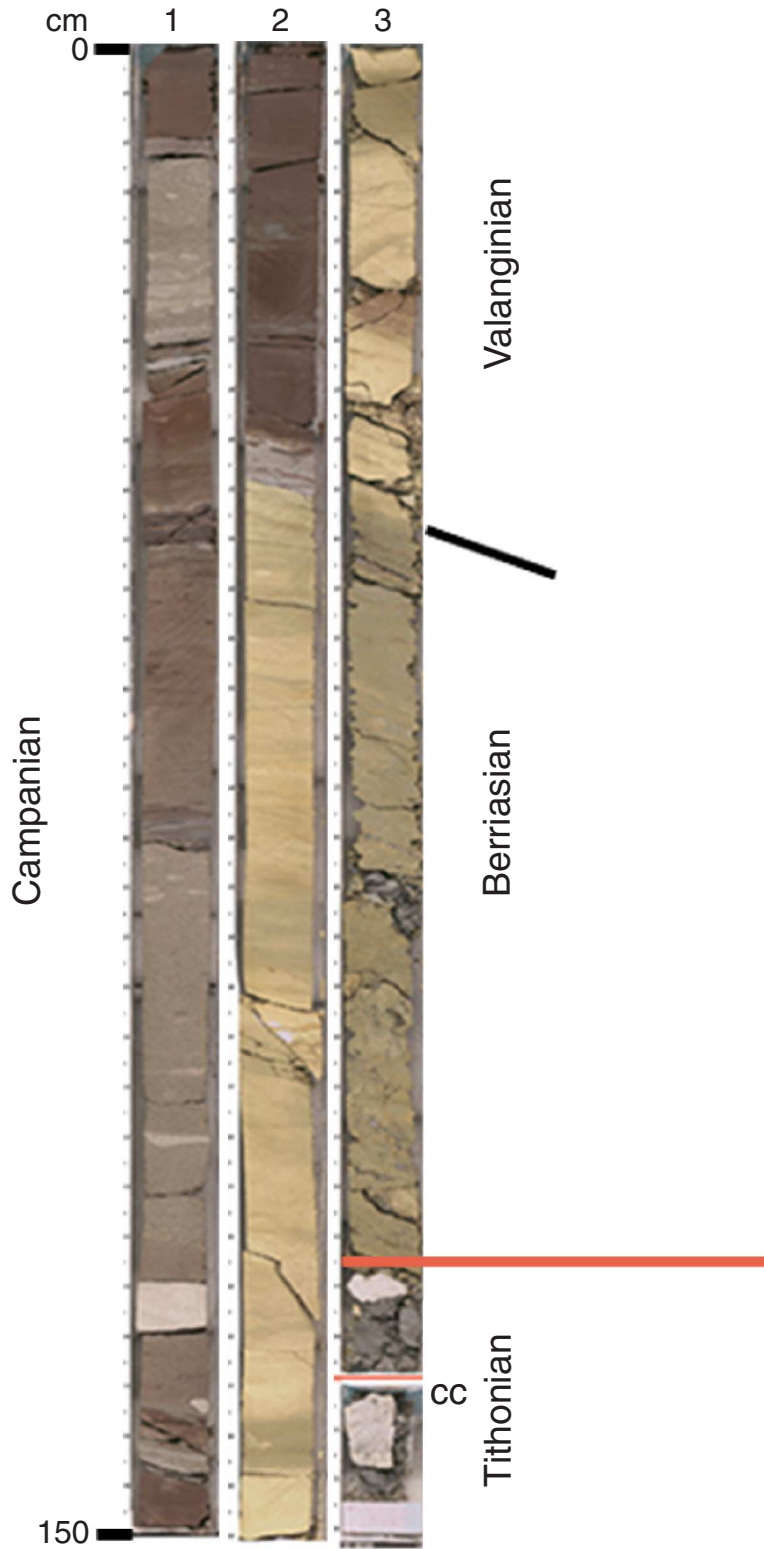
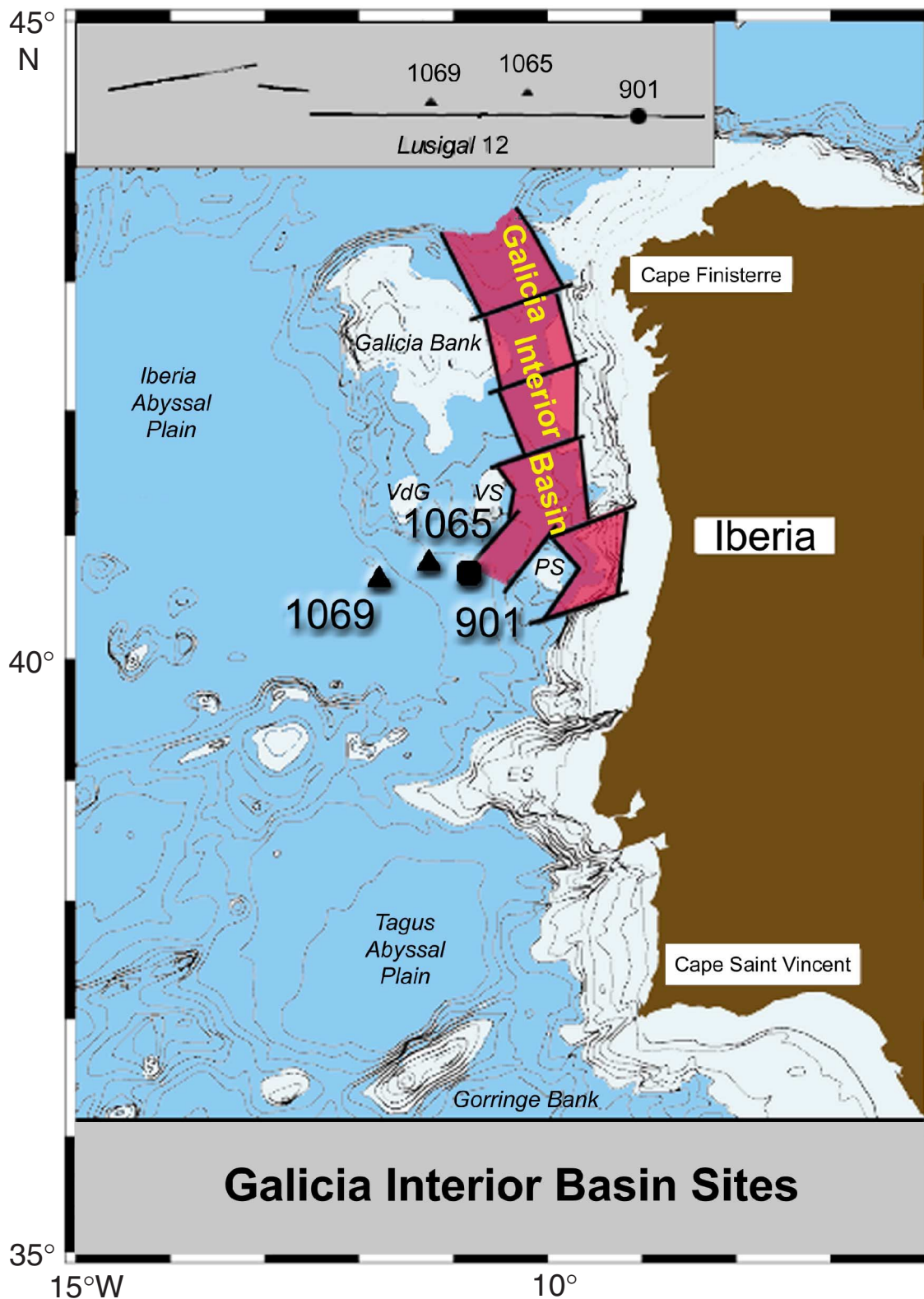
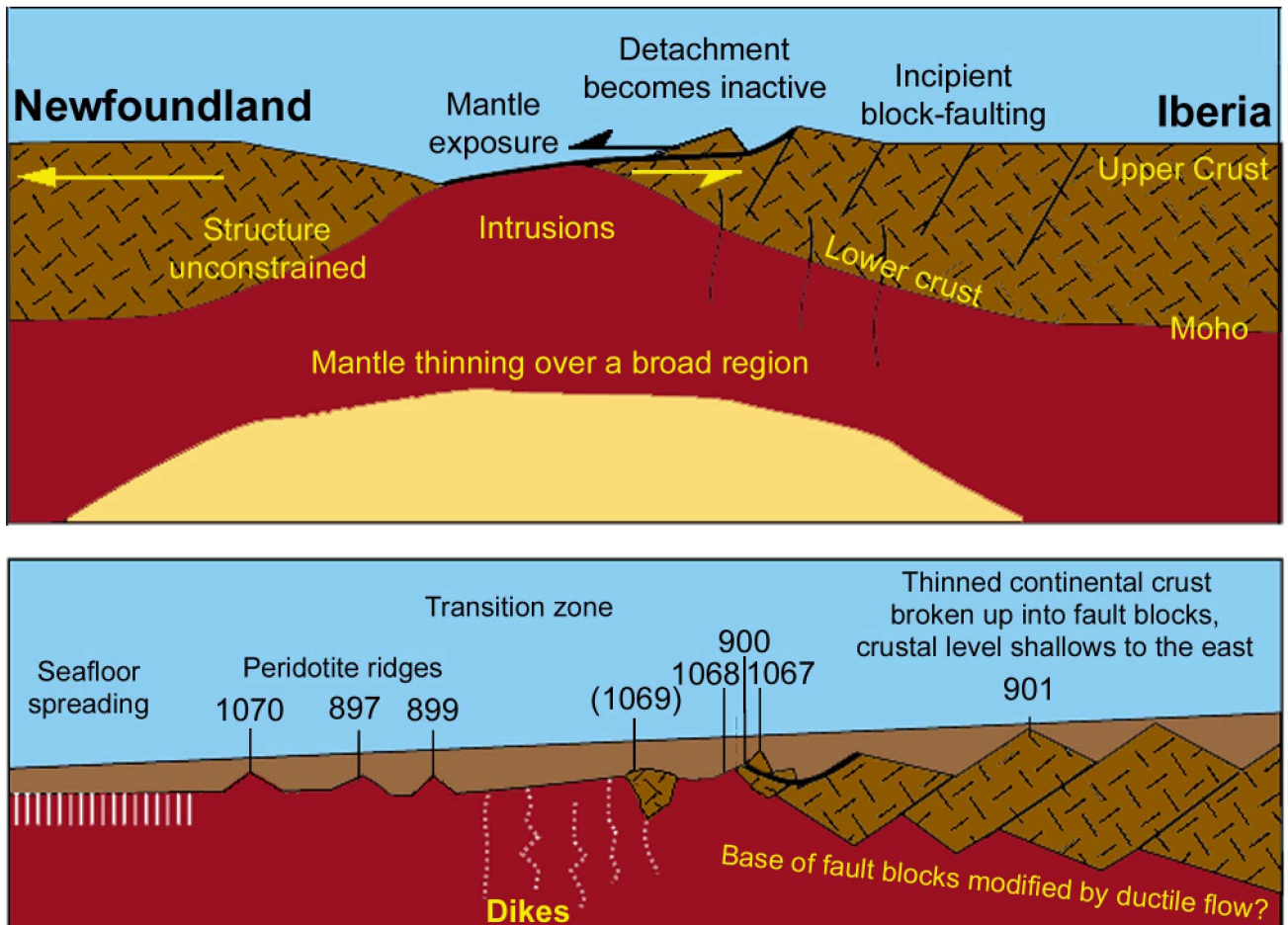


Figure F4. Locations of sites with Jurassic clastic sediments shown in relation to the Galicia interior basin (modified from Fig. F1, p. 12; approximate location of the Galicia Basin is from Pinheiro et al., 1996, fig. 5). Solid circle = ODP Leg 149 Site 901. Solid triangles = sites drilled during Leg 173.



**Figure F5.** Simplified model (after Krawczyk et al., 1996) to account for the dispersion of sites with Jurassic clastic sediments (Fig. F3, p. 14) by extension of the lithosphere through detachment faulting during rifting of the southern Iberia Abyssal Plain margin. A. In a first phase of rifting, lithospheric extension may have been accommodated by detachment faulting. B. Block-faulting subsequently cuts the upper plate into tilted blocks, dismembering the detachment system and the lower plate. Sites in parentheses are offset a short distance from the three seismic reflection profiles used to create the composite section (see inset, Fig. F2, p. 13).



Detachment Fault Model (after Krawczyk et al., 1996)



Table T2. Stratigraphic distribution of calcareous nannofossils from Hole 1069A.

Age	Core, section, interval (cm)	Depth (mbsf)	Abundance	Preservation	<i>Coccospheres</i> (various taxa)	<i>Axopodorhabdus cylindricus</i>	<i>Axopodorhabdus</i> sp.	<i>Conusphaera mexicana mexicana</i> (4-9 µm)	<i>Conusphaera mexicana minor</i>	<i>Corollithion</i> sp.	<i>Cruciolipsis cavillieri</i>	<i>Cyclagelosphaera deflandrei</i>	<i>Cyclagelosphaera margerellii</i>	<i>Diadorhombus rectus</i> *	<i>Diazomatoolithus galicianus</i>	<i>Diazomatoolithus lehmanii</i>	<i>Discorhabdus corollatus</i>	<i>Discorhabdus patulus</i>	<i>Ellipsagelosphaera britannica</i>	<i>Hexapodorhabdus cuvillieri</i>	<i>Microstaurus chiastius</i>	<i>Microstaurus quadratus</i>	<i>Paleopontosphaera dubia</i>	<i>Paleopontosphaera erismata</i>	<i>Polypodorhabdus escaigii</i>	<i>Stephanolithion bigotii</i>	<i>Stradnerolithus sexiramatus</i>	<i>Tubirhabdus patulus</i>	<i>Umbria granulosa minor</i>	<i>Watznaueria barnesae</i>	<i>Watznaueria ovata</i>	<i>Zeughrabdotus embergerii</i>	<i>Zeughrabdotus erectus</i>	
late Tithonian	173-1069A-16R-3, 129	867.90	A	G	C	R	R	F	R	P	R	F	F	P	R	F	R	R	C	P	R	P	F	F	R	P	R	R	R	R	A	R	R	R

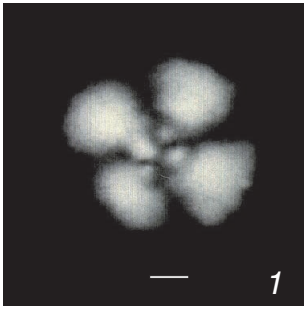
Notes: \* = may be a downhole contaminant. Abundance: A = abundant, C = common, F = few, R = rare, P = present. Preservation: G = good. Shaded cells = primary biostratigraphic index species.

**Table T3.** Size variations of *Watznaueria barnesae* from open marine (Site 869) and restricted paleoenvironments (Sites 873, 874, and 877 vs. Site 1065).

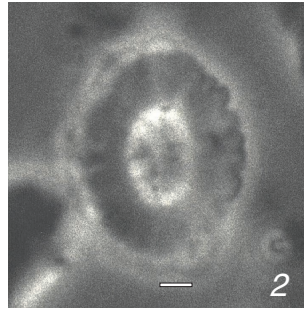
Specimens	Measured specimens (N)	Range (length vs. width in $\mu\text{m}$ )	Mean ( $\mu\text{m}$ )
Holotype*	NA	L = 5.5 W = 4.8	NA
Site 869, open marine*	30	L = 6-9 W = 5-7	NA
Sites 873, 874, 877, Campanian lagoonal sediments (Wodejebato Atoll)*	30	L = 3.5-4.4 W = 2.7-3.6	NA
Site 1065A, Tithonian restricted clastic basin	30	L = 5-9 W = 4-8	L = 6.8 W = 5.8

Notes: \* = From Erba et al. (1995, table 8). NA = not applicable.

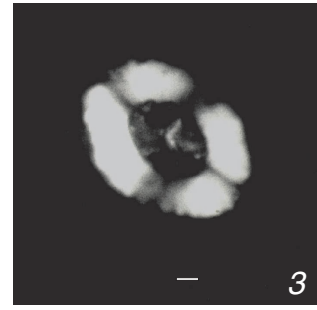
Plate P1. Light micrographs of calcareous nannofossils from Hole 1065A. Scale bars = 1  $\mu$ m.



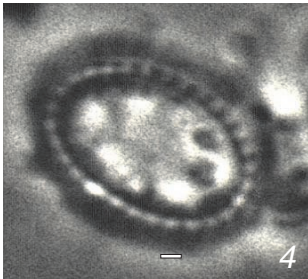
*Cyclagelosphaera margerelii*  
Distal view, Cross-polarized light.  
Sample 1065-11R-CC



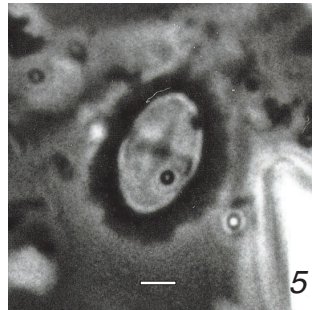
*Miravetesina favula*  
Distal view, Phase-contrast light.  
Sample 1065-13R-CC



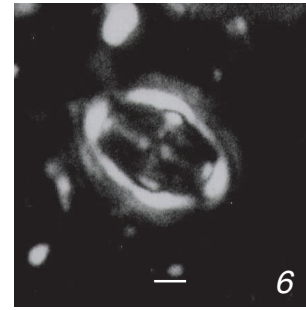
*Miravetesina favula*  
Distal view, Cross-polarized light.  
Sample 1065-13R-CC



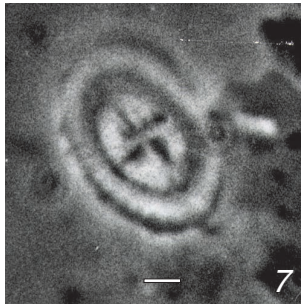
*Hexapodorhabdus cuvillieri*  
Distal view, Phase-contrast light.  
Sample 1065-15R-CC



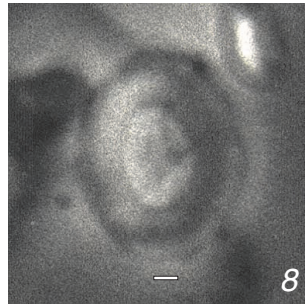
*Polypodorhabdus escaigii*  
Distal view, Phase-contrast light.  
Sample 1065-15R-CC



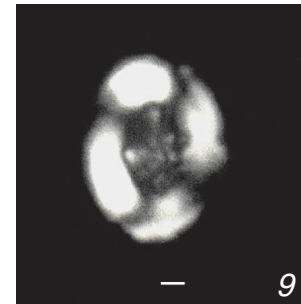
*Polypodorhabdus escaigii*  
Distal view, Phase-contrast light.  
Sample 1065-15R-CC



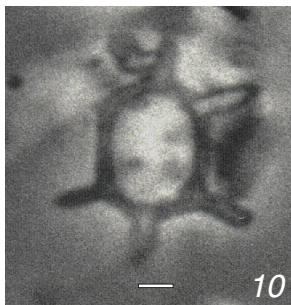
*Polypodorhabdus escaigii*  
Distal view, Cross-polarized light.  
Sample 1065-15R-CC



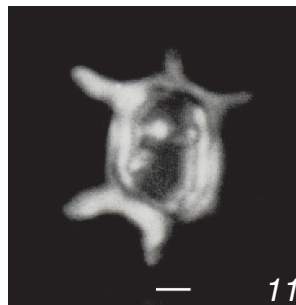
*Microstaurus chiastius*  
Distal view, Phase-contrast light.  
Sample 1065-15R-CC



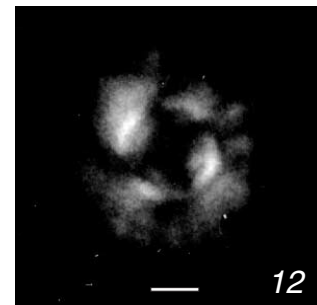
*Microstaurus chiastius*  
Distal view, Cross-polarized light.  
Sample 1065-15R-CC



*Stephanolithion bigotii* ssp. *bigotii*  
Distal view, Phase-contrast light.  
Sample 1065-15R-CC

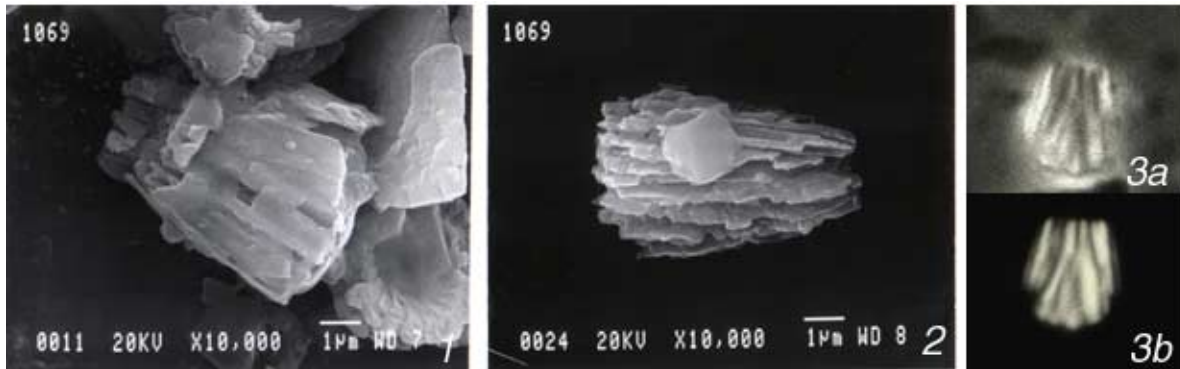


*Stephanolithion bigotii* ssp. *bigotii*  
Distal view, Cross-polarized light.  
Sample 1065-15R-CC



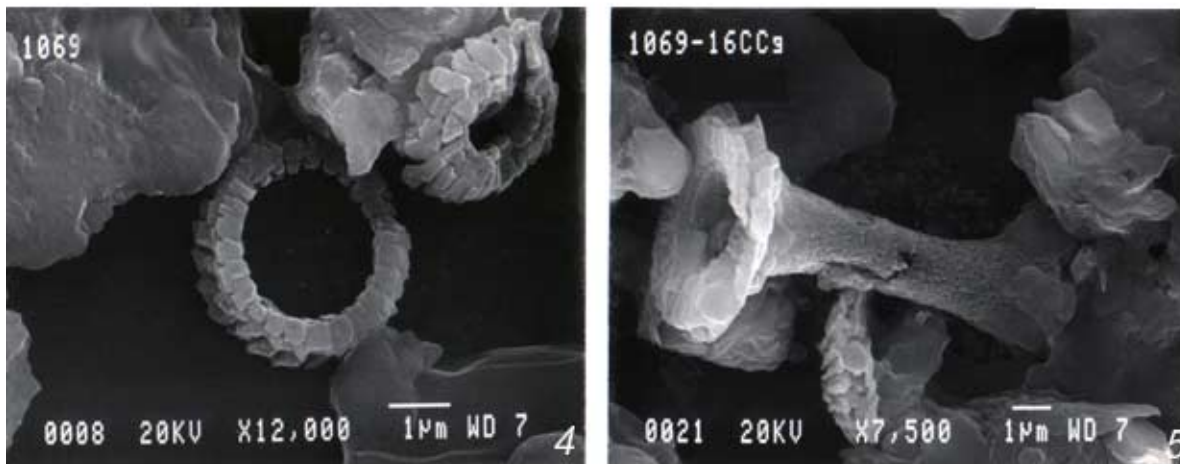
*Discorhabdus* sp.  
Distal view, Cross-polarized light.  
Sample 1065A-20R-CC

Plate P2. Scanning electron micrographs of calcareous nannofossils from Sample 173-1069A-16R-3, 129 cm, except for figure 3. 1, 2. Partially etched specimens showing inner cores of the conusphaerids. 3. (a) phase-contrast and (b) cross-polarized light micrographs of a specimen from Sample 173-1065A-11-CC, 14–16 cm. (figs. 2, 4, and 5 are from Wilson et al., in press.)



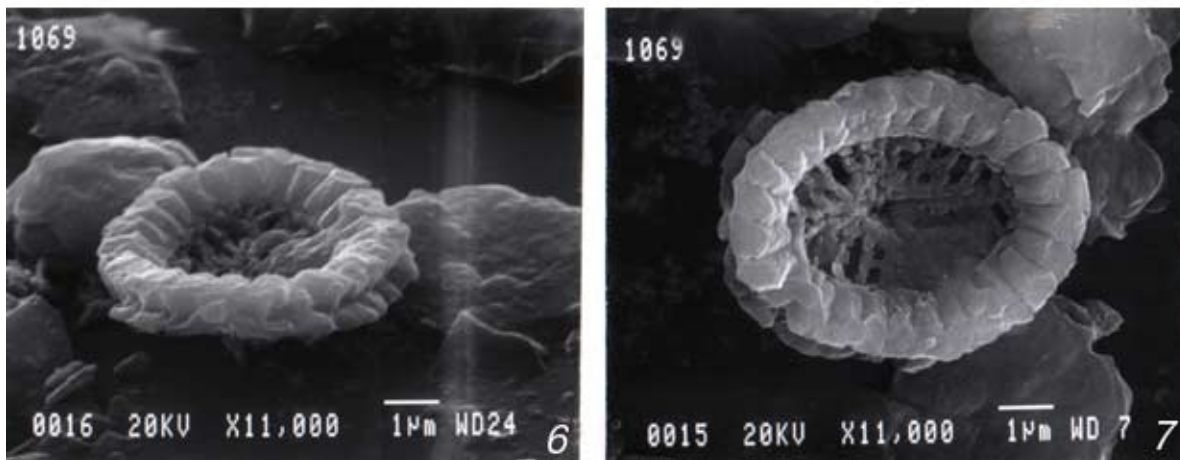
*Conusphaera mexicana mexicana*  
Lateral view

1 µm  
C. m. minor



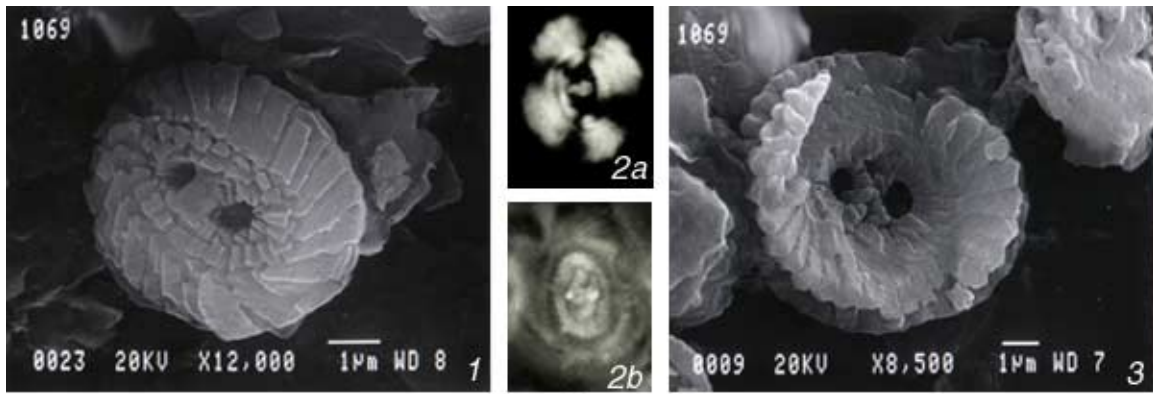
*Diazomatalithus galicianus*  
Proximal view

*Discorhabdus patulus*  
Lateral view



*Polypodorhabdus escaigii*  
Lateral and proximal views of the same specimen

Plate P3. Scanning electron micrographs of calcareous nannofossils from Sample 173-1069A-16R-3, 129 cm, except for figure 2, showing a moderate range of preservations. 1. Somewhat overgrown specimen. 2. (a) Cross-polarized and (b) phase-contrast light micrographs of a specimen from Sample 173-1065A-19R-CC, 7–8 cm. 3. Partially etched and slightly specimen. 4. *Ellipsagelosphaera britannica*, proximal view. 5. Essentially pristine specimen. 6. Etched specimens. 7. Overgrown specimens. (figs. 6 and 7 are from Wilson et al., in press)

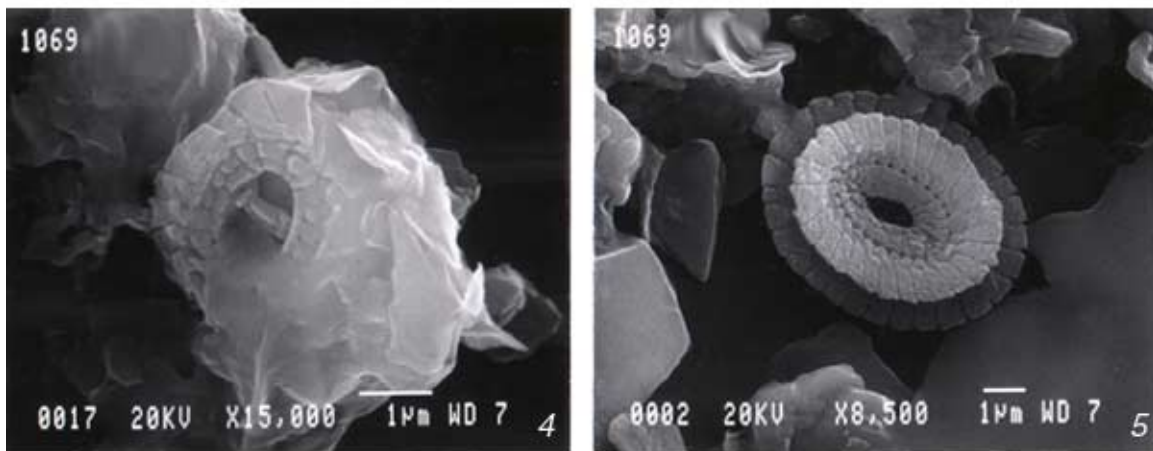


Distal view

1 µm

Proximal view

*Ellipsagelosphaera britannica*

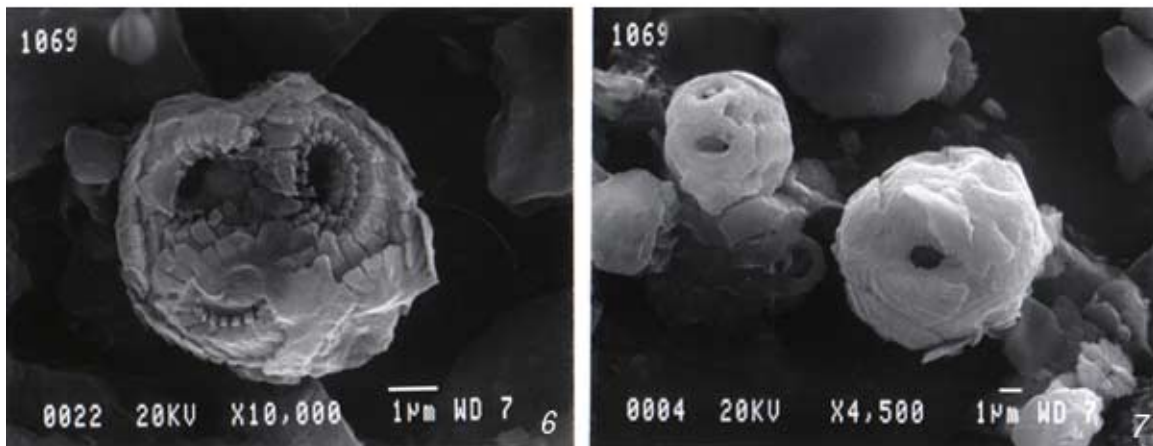


*Ellipsagelosphaera britannica*

Proximal view

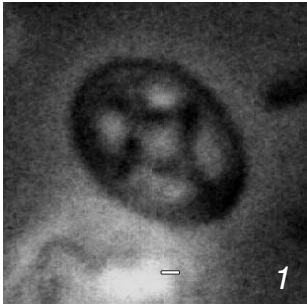
*Watznaueria barnesae*

Proximal view

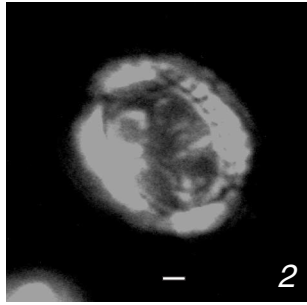


*Watznaueriacid coccospheres*

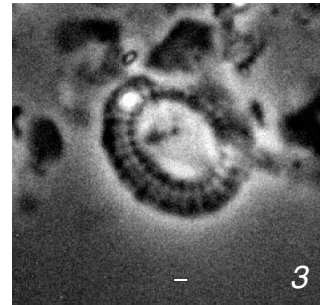
Plate P4. Light micrographs of calcareous nannofossils from Sample 173-1069A-16R-3, 129 cm. Scale bars = 1  $\mu\text{m}$ .



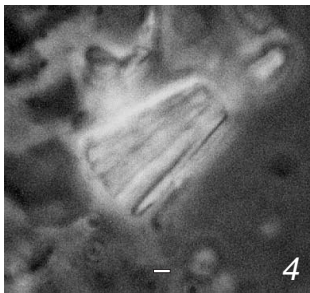
*Axopodorhabdus cylindratus*  
Distal view, Phase-contrast light.



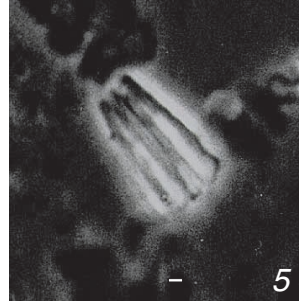
*Axopodorhabdus cylindratus*  
Distal view, Cross-polarized light.



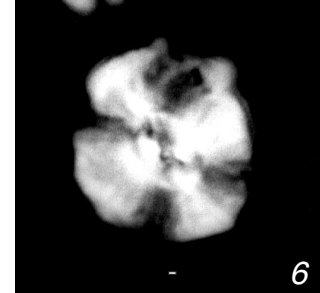
*Axopodorhabdus* sp.  
Proximal view, Phase-contrast light.



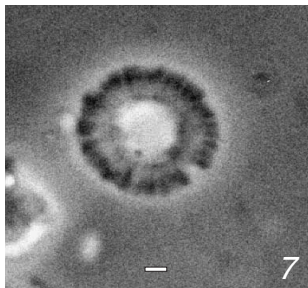
*Conusphaera mexicana*  
Side view, Phase-contrast light.



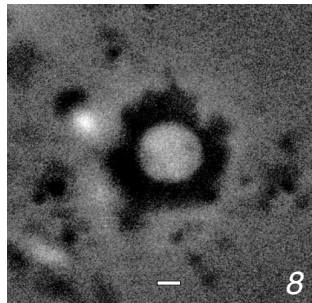
*Conusphaera mexicana* ssp. *mexicana*  
Distal view, Cross-polarized light.



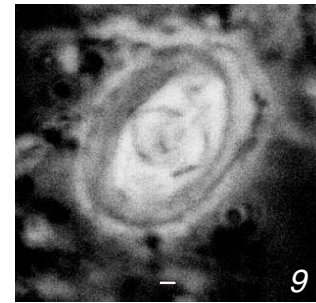
*Cyclagelosphaera deflandrei*  
Distal view, Cross-polarized light.



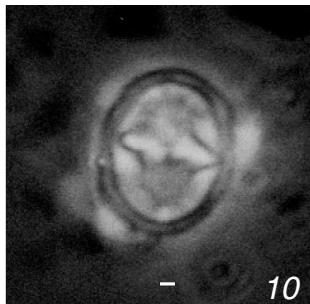
*Diazomatolithus galicianus*  
Proximal view, Phase-contrast light.



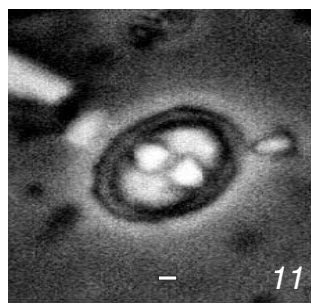
*Diazomatolithus lehmanii*  
Distal view, Phase-contrast light.



*Zeughrabdotos embergeri*  
Distal view, Cross-polarized light.

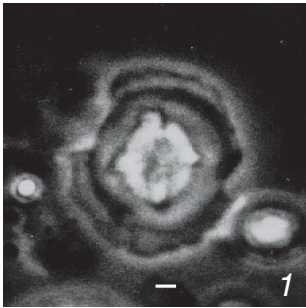


*Zeughrabdotos embergeri*  
Distal view, Phase-contrast light.

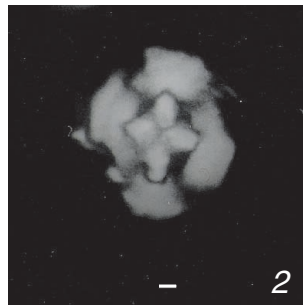


*Zeughrabdotos erectus*  
Distal view, Phase-contrast light.

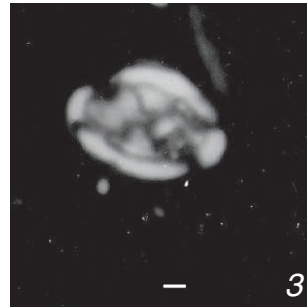
Plate P5. Light micrographs of *C. cuvillieri* and *U. granulosa* ssp. *minor* from Sample 173-1069A-16R-3, 129 cm. Scale bars = 1  $\mu$ m.



*Cruciellipsis cuvillieri*  
Proximal view, Phase-contrast light.



*Cruciellipsis cuvillieri*  
Proximal view, Cross-polarized light.



*Umbria granulosa* ssp. *minor*  
Distal view, Cross-polarized light.